

Relationship of nitrogen isotope fractionation to phytoplankton size and iron availability during the Southern Ocean Iron RElease Experiment (SOIREE)

K. L. Karsh

Antarctic Cooperative Research Centre, G.P.O. Box 252-80, Hobart, Tasmania 7001 Australia; Institute of Antarctic and Southern Ocean Studies, University of Tasmania, G.P.O. Box 252-77, Hobart, Tasmania 7001 Australia; Australian-American Fulbright Commission, P.O. Box 9541, Deakin, Australian Capital Territory 2600 Australia

T. W. Trull

Antarctic Cooperative Research Centre, G.P.O. Box 252-80, Hobart, Tasmania 7001 Australia

M. J. Lourey

Antarctic Cooperative Research Centre, G.P.O. Box 252-80, Hobart, Tasmania 7001 Australia; Institute of Antarctic and Southern Ocean Studies, University of Tasmania, G.P.O. Box 252-77, Hobart, Tasmania 7001 Australia

D. M. Sigman

Department of Geosciences, Guyot Hall, Princeton University, Princeton, New Jersey 08544

Abstract

The ^{15}N composition of sediments has been used as a proxy for nitrate utilization in surface waters to assess the role of Southern Ocean export production in glacial/interglacial changes in atmospheric CO_2 concentration. Interpretation has relied on a temporally constant isotope effect (ϵ) associated with uptake and assimilation of nitrate by phytoplankton. To investigate the reliability of this approach, we examined the relationships between the ^{15}N compositions of dissolved nitrate, bulk and size-fractionated (200, 70, 20, 5, 1 μm) suspended particulate organic nitrogen (PON), and sinking particles obtained from sediment traps during the Southern Ocean iron release experiment (SOIREE). We found variations in phytoplankton nitrogen isotopic compositions with both cell size and iron availability. $\delta^{15}\text{N}_{\text{PON}}$ increased by $>2\text{‰}$ with increasing size, both within and outside the iron-enriched patch. In comparison to unfertilized waters, $\delta^{15}\text{N}_{\text{PON}}$ within the iron-fertilized patch was a further 3–4% higher in those size fractions dominated by large diatoms (20–70, 70–200 μm). We speculate that this iron response might result from (1) variation in ϵ of nitrate utilization or (2) an iron-stimulated shift from ammonium-based to nitrate-based production. Comparing the $\delta^{15}\text{N}$ of the large diatom-dominated size fractions to the $\delta^{15}\text{N}$ of nitrate suggests relatively low ϵ values of 4–5‰, in contrast to estimated values of 7–10‰ from seasonal nitrate depletion and export production. This suggests that higher glacial $\delta^{15}\text{N}$ in Southern Ocean sediments could, in part, reflect increases in iron availability, dominant cell size, and possibly growth rates, and these effects must be considered in any quantitative scaling of $\delta^{15}\text{N}$ variations, including those of diatom-bound $\delta^{15}\text{N}$, to the extent of nitrate utilization.

The nitrogen isotopic composition of sediments has been used as a palaeoproxy for nitrate utilization in the Southern Ocean to investigate the region's role in driving glacial/interglacial changes in atmospheric CO_2 composition (François et al. 1992, 1997; Sigman et al. 1999a). Increased nutrient utilization in the glacial Southern Ocean could be linked to lower atmospheric CO_2 through changes in the efficiency of the biological pump, or reduced nutrient supply and release of CO_2 to the atmosphere (e.g., Kumar et al. 1995; François et al. 1997 and references therein). Ni-

trogen isotope data from the Antarctic region of the Southern Ocean suggests that nitrate utilization in the glacial Southern Ocean was twice the current value, supporting a significant role for the region in lowering glacial atmospheric CO_2 concentrations (François et al. 1997; Sigman et al. 1999a). The nitrogen isotopic composition of sediments provides a proxy of the fractional extent of nutrient utilization but must be combined with models of export and supply to provide information on the mechanism leading to changes in utilization or the resulting effect on extent of CO_2 sequestration or degassing.

Both field-based and culture studies (*see* references in Sigman et al. 1999a) have demonstrated that the isotopic composition of particulate organic nitrogen (PON) can be used as a proxy for the extent of nitrate utilization. Isotopic fractionation during nitrate uptake by organic matter leads to preferential incorporation of ^{14}N relative to ^{15}N into phytoplankton cells. As the nitrate supply is consumed and fractionated, the nitrate in surface waters becomes progressively

Acknowledgments

This work was made possible by the generous and professional efforts of all the SOIREE participants. Discussion with R. François and L. Armand provided important insights. The comments of M. Altabet, W. Howard, and an anonymous reviewer improved the paper. We thank R. Ho and G. Cane for assistance with nitrate isotope analyses. K. Karsh's participation in this work was supported by an Australian-American Fulbright fellowship. D. Sigman was supported by grant OCE00-81686 from the U.S. NSF Ocean Sciences.

enriched in ^{15}N , producing a subsequent increase in the ^{15}N content of newly formed PON. Thus, increased nitrate utilization is reflected in an increase in $\delta^{15}\text{N}_{\text{PON}}$ of suspended and sinking particles and, ultimately, in sediments (e.g., François et al. 1992; Altabet and François 1994).

A major uncertainty associated with use of the nitrogen isotope palaeoproxy is potential variation in the isotope effect (ϵ) associated with nitrate utilization by phytoplankton (Altabet and François 1994; Sigman et al. 1999b). Temporal variations in the isotope effect could lead to changes in the isotopic composition of the sinking nitrogen flux that would be erroneously interpreted as changes in the extent of nitrate utilization. Surprisingly few studies have addressed potential controls on the isotope effect accompanying nitrate assimilation such as cell size and growth rate. Iron availability is another potential control on the nitrogen isotope effect, as nitrate assimilation is catalyzed by two iron-containing enzymes, and accumulating evidence suggests iron availability partially controls phytoplankton community composition in the Southern Ocean (*see* review in de Baar and Boyd 1999).

To investigate potential relationships between the isotope effect of nitrate utilization and iron availability, cell size, and growth rate, this study examined relationships between the ^{15}N compositions of bulk and size-fractionated suspended PON, sinking particles, and dissolved nitrate during the Southern Ocean Iron RElease Experiment (SOIREE). We found evidence for variation in nitrogen isotopic compositions with both cell size and iron availability, results that could affect quantitative scaling of the $\delta^{15}\text{N}$ palaeoproxy to past nitrate utilization in the Southern Ocean.

Methods

Oceanographic setting—SOIREE was carried out at 61°S 140°E south of Australia in late summer. The experiment took place in a moderately deep mixed layer (~ 65 m) in the presence of abundant dissolved nitrate, phosphate, and silicate (~ 25 , 1.5 , and $10 \mu\text{mol L}^{-1}$, respectively), although considerable seasonal nutrient depletion had already occurred (Trull et al. 2001).

Surface waters were fertilized with iron as acidified $\text{FeSO}_4 \cdot 7\text{H}_2\text{O}$ and sulfur hexafluoride (SF_6) as a tracer on day 1 (defined as the 24-h period starting at 0100 h, 10 February 1999 NZST), and again with iron alone on days 3, 5, and 7. Monitoring of the patch consisted of daily underway mapping of the iron and SF_6 tracer and CTD and pump sampling of the center of the fertilized area, as defined by the SF_6 tracer. Waters outside the fertilized area were sampled less frequently, and because of ship logistics, the location of out-patch hydrographic stations varied relative to the patch center. Possible spatial variability in out-patch samples should be kept in mind in assessing any temporal changes. Ship-board monitoring ceased on day 13, 22 February 1999. The iron fertilization induced an almost sixfold increase in phytoplankton biomass (based on chlorophyll *a* [Chl *a*]), a floristic shift from picoplankton to large diatoms (Gall et al. 2001a), and an approximate doubling of PON within the mixed layer over the observation period, but essentially no changes below the mixed layer (Gall et al. 2001a). An over-

view of SOIREE is available (Boyd et al. 2000), and many aspects have been described in detail in a dedicated volume of Deep-Sea Research II (48(11–12), 2001).

Dissolved nitrate ^{15}N analyses—All ^{15}N analyses are presented in the delta (δ) notation in parts per thousand (‰) relative to atmospheric N_2 : $\delta^{15}\text{N} = [({}^{15}\text{N}/{}^{14}\text{N})_{\text{sample}}/({}^{15}\text{N}/{}^{14}\text{N})_{\text{atm}} - 1] \times 1,000$. The isotopic effect accompanying nitrate utilization is presented in the epsilon notation (ϵ , also in parts per thousand) which describes the fractionation accompanying a chemical transformation: $\epsilon = (k^{14}/k^{15} - 1) \times 1,000$, where k^{14}/k^{15} is the ratio of the specific reaction rates for ^{14}N and ^{15}N .

Three depth profiles collected from the CTD/Niskin Rosette system were selected for nitrate nitrogen isotopic composition analysis: (1) day 3 within the patch, which provides the first $[\text{NO}_3^-]$ data available and is considered representative of initial conditions because little change in beam attenuation, primary productivity rates, column-integrated Chl *a*, or mean biovolume had occurred from day 0, (2) day 12 from outside the patch late in the experiment, and (3) day 13 from within the patch late in the experiment. Nutrient concentrations were measured by another group (Frew et al. 2001). Samples for $\delta^{15}\text{N}_{\text{NO}_3}$ were filtered through GF/F glass fiber filters at low pressure using a Teflon and glass system, acidified to $\text{pH} < 2$ with $5 \mu\text{l ml}^{-1}$ 50% phosphoric acid, and stored refrigerated in the dark until analysis.

Nitrate nitrogen isotopic compositions were determined using the “denitrifier method”—a microbial conversion of the sample nitrate to N_2O followed by isotopic analysis of the N_2O product by continuous flow isotope ratio mass spectrometry (Sigman et al. 2001). The isotopic composition of the N_2O was measured relative to N_2O from a gas cylinder. Referencing to atmospheric N_2 was by comparison to replicates of the KNO_3 reference material IAEA-N3 ($\delta^{15}\text{N} = 4.7\text{‰}$) processed with each batch of samples. Replication of samples and the reference material indicated a precision of $\pm 0.2\text{‰}$ ($\pm \text{SD}$) or better, as reported previously for this method.

Particle ^{15}N analyses—Three types of particle samples were obtained and analyzed for their N content and isotopic composition: bulk suspended particles, size-fractionated suspended particles, and sinking particles. Suspended particles were collected via a high-volume submersible pump within and outside the patch from 10, 30, 65, and 100 m (bulk) and 30 and 100 m (size fractionated). Sinking particles were collected using trap arrays deployed at ~ 110 m. Full details of the collection procedures for these samples are presented in Trull and Armand (2001 and references therein). The size fractions were examined by light microscopy; representative counts of relative percent abundances and a complete list of the species encountered can also be found in Trull and Armand (2001).

$\delta^{15}\text{N}$ analysis of particle samples was conducted using a Finnagin Delta-S IRMS coupled with a Carlo Erba/Fisons 1108 elemental analyzer (EA) via a ConFlo II interface. All samples were sealed in pre-cleaned lightweight tin cups for analysis. The pellets were combusted in a stream of oxygen at an oven temperature of $1,190^{\circ}\text{C}$ in narrow-bore quartz

tubes (9 mm) packed with silica chips, CuO, WO₃, and silver wire and passed over hot copper at 650°C to yield N₂ gas (modifications to the Carlo Erba methods are similar to those of L. A. Houghton, C. G. Johnson, D. J. Repeta, and S. Pantoja, pers. comm.). H₂O and CO₂ were removed from the gas stream using magnesium perchlorate and soda lime. The narrow tubes increased the peak height about threefold and improved the precision for δ¹⁵N measurements on samples a few micromoles of N in size.

For calibration, a laboratory working standard ML-N₂ (ultra-high purity N₂) was injected before and after each sample. The standard was calibrated against purified atmospheric N₂ using dual-inlet infrared isotope ratio mass spectroscopy (IRMS). In addition, IAEA standards IAEA-N1 ((NH₄)₂SO₄, δ¹⁵N = 0.43 ± 0.07‰) and IAEA-N3 (KNO₃, δ¹⁵N = 4.72 ± 0.13‰) were run with each set of analyses. The standards gave a precision of 0.14‰ for IAEA-N1 (*n* = 77) and 0.16‰ for IAEA-N3 (*n* = 52). A correction value was added to sample δ¹⁵N results based on the offset between the measured δ¹⁵N of standards and their specified values during each analysis period (samples were run in three groups separated by 2–3 months; correction values were 0.38‰, 0.33‰, and 0.35‰, respectively). Precision of replicate samples was better than 0.3‰ within and across analysis periods. Organic C:N ratios were also analyzed using an elemental analyzer following the methods detailed in Lourey and Trull (2001). Precision for working standards was better than 1%, but sample reproducibility was limited by the filter subsampling and is typically closer to ~10% for concentrations and ~5% for POC:PON ratios. Unfortunately, the ship schedule and sampling methods precluded sampling size-fractionated and bulk particles on the same day. Comparing samples from similar stages of the experiment showed a variation of ±1‰ between summed size fraction δ¹⁵N_{PON} and bulk δ¹⁵N_{PON}. This difference might be attributable to changes in the water column between sampling days. However, it is possible that the sampling techniques affected the δ¹⁵N_{PON} values of the size fractions. Summed size fraction PON concentrations were typically half of the bulk PON values, suggesting that filtering of the size fractionated samples led to low sample concentration.

Results and interpretation

Nitrate concentrations and isotopic compositions—Considerable seasonal depletion of nitrate in the summer-warmed surface mixed layer had already occurred at the start of SOIREE, as shown by the vertical profiles in Fig. 1. The temperature minimum layer (*T*_{min}) at 100–120 m is characteristic of the cold wintertime mixed layer that has been capped by the warmer summertime mixed layer; as such, the *T*_{min} provides an estimate of the [NO₃⁻] and δ¹⁵N_{NO₃} composition prior to spring and summer phytoplankton growth. From the *T*_{min} (or winter) nitrate concentration of 29.7 μmol L⁻¹ and δ¹⁵N_{NO₃} of ~5.6‰, mixed-layer (30–40 m) nitrate concentrations had been depleted to 25.0 μmol L⁻¹, and δ¹⁵N_{NO₃} had risen to ~7.2‰ by seasonal phytoplankton growth by the start of SOIREE (Fig. 1). Similar mixed-layer nitrate depletion and ¹⁵N_{NO₃} enrichment were also observed

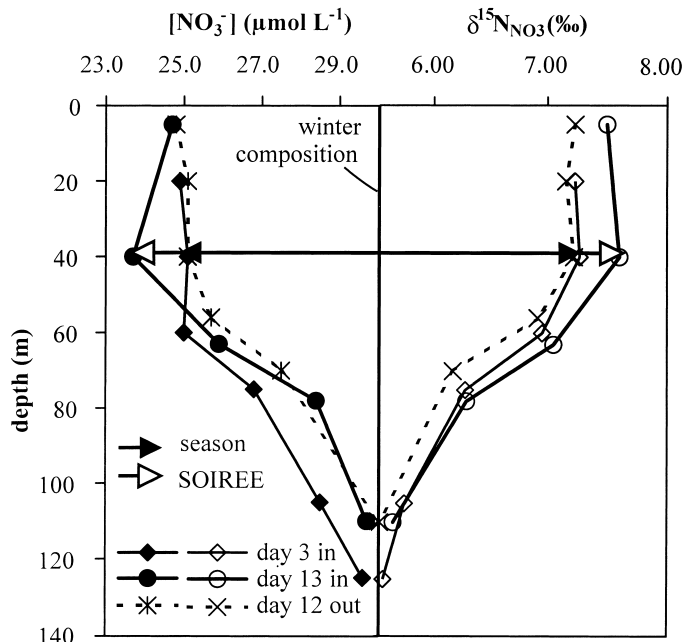


Fig. 1. Depth profiles of [NO₃⁻] and δ¹⁵N_{NO₃}. Mixed layer depth remained ~65 m throughout SOIREE. At the beginning (day 3), mixed-layer nitrate was already depleted in concentration and enriched in ¹⁵N by seasonal uptake in comparison to winter conditions (preserved in the remnant temperature-minimum layer at ~110 m). SOIREE produced a small additional depletion (~25% of total) by day 13. Precision of δ¹⁵N_{NO₃} measurements was 0.2‰. [NO₃⁻] values are from Frew et al. (2001) and R. Frew (pers. comm.).

outside the iron-fertilized patch (Table 1 in Web Appendix 1 at <http://www.aslo.org/lo/toc/vol48/issue3/1058a1.pdf>). The iron-induced algal bloom caused a further mixed-layer nitrate depletion of 1.3 μmol L⁻¹ (R. Frew pers. comm.; Frew et al. 2001) and a δ¹⁵N_{NO₃} increase of 0.5‰ over the 13 d of observation (as shown by the profiles for day 13 in Fig. 1).

The nitrogen isotopic fractionation accompanying the seasonal nitrate depletion observed can be estimated by fitting the data to the Rayleigh fractionation equation for a closed system experiencing nitrate removal with constant accompanying isotopic fractionation, denoted by ε,

$$\delta^{15}\text{N}_{\text{NO}_3} = \delta^{15}\text{N}_{\text{NO}_3\text{initial}} - \varepsilon \ln(1 - u) \quad (1)$$

where $u = ([\text{NO}_3^-]_{\text{initial}} - [\text{NO}_3^-]) / [\text{NO}_3^-]_{\text{initial}}$, or the fraction of the nitrate pool utilized. The vertical profiles both inside and outside the SOIREE iron-fertilized waters conform reasonably well to this relation. The profiles from days 3, 12, and 13 suggest values of ε = 10.0 ± 1.2‰, 9.5 ± 1.2‰, and 8.9 ± 1.1‰ with *r*² values of 0.98, 0.98, and 0.99, respectively. The three estimates yield an uncertainty weighted mean and standard error (2σ) of 9.4 ± 0.9‰. Unfortunately, the SOIREE-induced nitrate depletion and δ¹⁵N_{NO₃} increase was too small to permit separate estimation of the isotopic fractionation accompanying nitrate uptake during the SOIREE bloom from the seasonal effect.

An ε = 9.4 ± 0.9‰ is at the high end of the range of previous field-based estimates of the isotope fractionation

effect of nitrate uptake (4–9‰), in particular by comparison to early estimates for the Southern Ocean of 4–6‰ (Sigman et al. 1999b). Altabet and François (2001) recently estimated a similarly high $\epsilon = 8.2\text{‰}$ for the Antarctic Zone at 190°E using both summertime depth profiles and seasonal variations in the mixed layer. Our higher estimates arise partially because summertime surface $\delta^{15}\text{N}$ values are $\sim 0.5\text{‰}$ higher for a given nitrate concentration in the Antarctic south of Australia (D. Sigman, M. Lourey, and T. Trull unpubl. data) than in the eastern Indian Pacific sector (Sigman et al. 1999b). However, as with the results of Altabet and François (2001), our higher epsilon estimates relative to earlier studies are also partly due to the choice of “initial” values of $[\text{NO}_3^-]$ and $\delta^{15}\text{N}_{\text{NO}_3}$. The higher estimates in Altabet and François (2001) and this study use initial values from the T_{min} layer, whereas the study resulting in $\epsilon = 4\text{--}6\text{‰}$ used values from a deeper source, owing to concerns that the T_{min} layer could have experienced alteration of NO_3^- and $\delta^{15}\text{N}_{\text{NO}_3}$ from remineralization. Nitrate in the T_{min} layer during SOIREE showed no evidence of seasonal remineralization inputs; it was identical to winter mixed-layer concentrations measured in earlier years at the SOIREE site (Trull et al. 2001).

These estimates of isotopic fractionation all derive from the simple closed-system description of Eq. 1. Although the simple closed-system description is clearly incomplete, it can be used with reasonable confidence with the relatively low nitrate utilization (typically 20%) experienced in the Southern Ocean; there is little difference in the determination of ϵ between open and closed systems at high and low values of u (Sigman et al. 1999b; Altabet and François 2001). Because any resupply of nitrate would require a higher value of ϵ to produce the observed $\delta^{15}\text{N}_{\text{NO}_3}$ increase, our estimate of ϵ using a closed system is a minimum. Our estimate of ϵ for the SOIREE region using $[\text{NO}_3^-]$ and $\delta^{15}\text{N}_{\text{NO}_3}$ is supported by applying the instantaneous product equation derived from Rayleigh fractionation kinetics to the pre-iron fertilization suspended and sinking particle $\delta^{15}\text{N}_{\text{PON}}$ (discussed further below). Epsilon values calculated in this way are $\sim 9\text{‰}$ (suspended $\delta^{15}\text{N}_{\text{PON}}$) and $\sim 7\text{--}8\text{‰}$ (sinking $\delta^{15}\text{N}_{\text{PON}}$). The lower isotope effect provided by the sinking flux number suggests that the nitrate-based isotope effect might be too high. Given this and the considerations discussed above, a range of 7–10‰ is consistent with the results of this study and appears to be a reasonable estimate for ϵ for seasonal nitrate depletion at the Antarctic Zone SOIREE site.

Bulk suspended particle ^{15}N composition—Bulk suspended particle $\delta^{15}\text{N}_{\text{PON}}$ values generally ranged between -3 and 1‰ throughout SOIREE. All vertical profiles, both inside and outside the iron-enriched patch, revealed ^{15}N -enriched particle compositions at middepth (30 m) within the surface mixed layer and below the mixed layer at 100 m (representative profiles are shown in Fig. 2 and complete data are in Table 2 in Web Appendix 1). Compared to outside the patch, in-patch samples were generally more ^{15}N -rich, and the 30-m and submixed-layer enrichments were more pronounced. The submixed-layer ^{15}N enrichment has been observed in previous studies and attributed to isotopic fractionation accompanying remineralization (e.g., Saino and Hattori 1980;

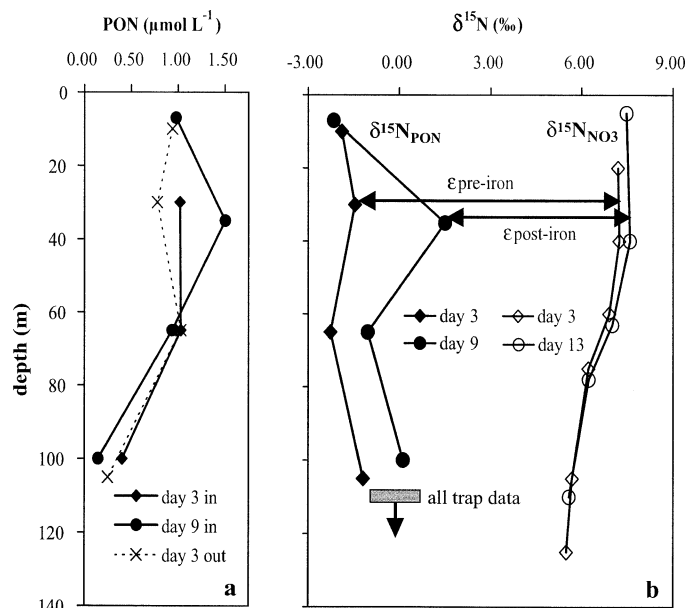


Fig. 2. (a) Iron-induced PON increase and (b) bulk suspended particle $\delta^{15}\text{N}_{\text{PON}}$ increase during SOIREE. Maximum PON accumulation and maximum bulk $\delta^{15}\text{N}_{\text{PON}}$ increase during the bloom occurred middepth ($\sim 30\text{--}40$ m) within the mixed layer. The large mixed-layer increase in $\delta^{15}\text{N}_{\text{PON}}$ ($\sim 3\text{‰}$) relative to the increase in $\delta^{15}\text{N}_{\text{NO}_3}$ ($\sim 0.5\text{‰}$) changes the offset between the two parameters, suggesting a change in the isotope effect (ϵ) of phytoplankton nitrate uptake. Sinking particle $\delta^{15}\text{N}_{\text{PON}}$ remained near 0‰ throughout SOIREE, consistent with observations of little to no iron-induced export during the 13 d of monitoring. Sinking particle $\delta^{15}\text{N}_{\text{PON}}$ was offset from $\delta^{15}\text{N}_{\text{NO}_3}$ by 7–8‰, slightly lower than the estimate of $\epsilon = 9.4 \pm 0.9\text{‰}$ from the Rayleigh model. Precision of suspended and sinking $\delta^{15}\text{N}_{\text{PON}}$ values is 0.3‰ , and precision of PON values is $0.1 \mu\text{mol L}^{-1}$. See Fig. 1 for precision of $\delta^{15}\text{N}_{\text{NO}_3}$ values.

Altabet and McCarthy 1986). There is perhaps some slim evidence for submixed-layer remineralization effects in the slightly elevated POC:PON ratios we observed below the mixed layer in both bulk and size-fractionated particles; POC:PON ratios tend to increase with remineralization as N is remineralized preferentially to C.

Within the in-patch mixed layer, the depth of maximal $\delta^{15}\text{N}_{\text{PON}}$ at 30 m corresponds to the depth of maximal primary production (Gall et al. 2001b) and maximal PON concentration (Fig. 2). At this depth, $\delta^{15}\text{N}_{\text{PON}}$ increased over time by $\sim 2\text{‰}$ in the iron-fertilized waters, with a maximum on day 9 of the 13-d observation period (Fig. 3). This temporal change in $\delta^{15}\text{N}_{\text{PON}}$ corresponds to the temporal increase in PON and Chl *a* concentration observed at the same depth (Fig. 3). The temporal increase in $\delta^{15}\text{N}_{\text{PON}}$ was about four times larger than the increase of $\sim 0.5\text{‰}$ of $\delta^{15}\text{N}_{\text{NO}_3}$ in the mixed layer (at 40 m) over the same period (Fig. 2). This disparity contrasts with the expectation from Rayleigh fractionation kinetics that new PON (the instantaneous product, PON-in) will increase in parallel with that of the source nitrate, offset by the isotopic fractionation factor for nitrate uptake (e.g., Sigman et al. 1999b; Altabet and François 2001):

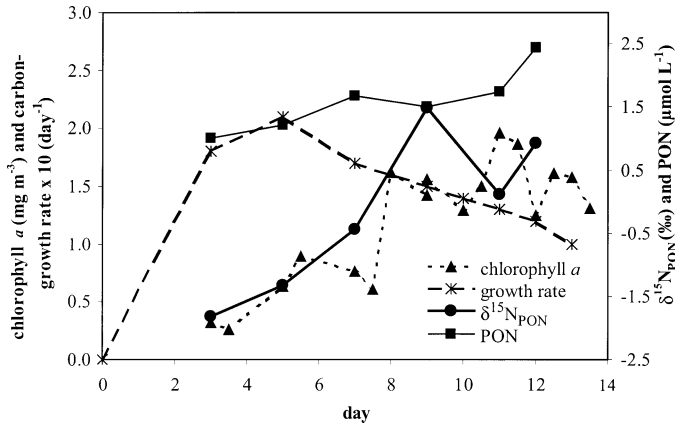


Fig. 3. Thirty-meter bulk $\delta^{15}\text{N}_{\text{PON}}$ temporal increase in comparison to biomass and growth rate changes. $\delta^{15}\text{N}_{\text{PON}}$ and Chl *a* peak near day 9–10 of SOIREE. PON concentrations increase steadily. Community growth rate peaks earlier (about day 5), suggesting a lag period between growth rate increases and change in isotopic composition. See Fig. 2 for precision of PON and $\delta^{15}\text{N}_{\text{PON}}$ values. Chl *a* and growth rate values are from Gall et al. 2001a.

$$\delta^{15}\text{N}_{\text{PON-in}} = \delta^{15}\text{N}_{\text{NO}_3} - \varepsilon \quad (2)$$

and that accumulating PON (PON-ac) will increase by even less.

$$\delta^{15}\text{N}_{\text{PON-ac}} = \delta^{15}\text{N}_{\text{NO}_3} + \varepsilon(1/u)\ln(1 - u) \quad (3)$$

(In Eq. 3, the term modifying ε is negative and >1 , and $\delta^{15}\text{N}_{\text{NO}_3}$ denotes the concurrent nitrate isotopic composition.) Both of these equations describe a single population of PON, but SOIREE included an evolving combination of the initial mix of slowly growing phytoplankton and detritus with the iron-induced phytoplankton production. Assuming that the initially present PON (day 3) was being removed slowly with a residence time of ~ 10 d (primarily via respiration at 10% of the initial production rate, as removal by sinking [Nodder and Waite 2001] and de-entrainment [Hannon et al. 2001] was minimal), would suggest that the newly forming PON might have had $\delta^{15}\text{N}_{\text{PON-in}}$ as high as 2.9‰. Although the exact nitrogen isotopic composition of the newly formed PON cannot be calculated with certainty, it is clear that the observed bulk values are minimum estimates of the $\delta^{15}\text{N}$ of new PON and, as such, provide minimum estimates of any changes in nitrogen metabolism induced by the fertilization. Pre-iron suspended $\delta^{15}\text{N}_{\text{PON}}$ values yield an epsilon estimate of $\sim 9\text{‰}$ when substituted in the instantaneous product equation, supporting our estimate of seasonal epsilon for the region from changes in $[\text{NO}_3^-]$ and $\delta^{15}\text{N}_{\text{NO}_3}$.

The $\delta^{15}\text{N}_{\text{PON}}$ increased by much more than $\delta^{15}\text{N}_{\text{NO}_3}$, suggesting that (1) iron induced a decrease in the ε of the phytoplankton nitrate uptake; (2) iron induced other changes in the phytoplankton population that led to increased $\delta^{15}\text{N}_{\text{PON}}$, the most likely being a shift from ammonium-based to nitrate-based production; or (3) the comparison of PON and nitrate isotopic compositions is biased by some other effect of the fertilization not driven by iron (e.g., entrainment of new nitrate or isotopically different PON into the patch). The last possibility appears unlikely because exchange with sur-

rounding waters was very small, $\sim 0.03 \text{ d}^{-1}$ (Hannon et al. 2001), and is not discussed further. The other two explanations of the nitrogen isotopic changes are discussed in detail below, after examining additional insights gained from the $\delta^{15}\text{N}_{\text{PON}}$ of the sediment trap and the size-fractionated suspended particles.

Sinking particle ^{15}N compositions—Sinking particles trapped at 110 m at the start of SOIREE both in and outside the iron-fertilized waters exhibited $\delta^{15}\text{N}_{\text{PON}}$ values near 0‰ (Fig. 2 and Table 3 in Web Appendix 1). The sinking PON values are slightly ^{15}N enriched in comparison to suspended PON in the mixed layer, a relationship that has been observed before (e.g., Altabet 1988). The smaller difference between the sinking $\delta^{15}\text{N}_{\text{PON}}$ and $\delta^{15}\text{N}_{\text{NO}_3}$ ($\sim 7\text{--}8\text{‰}$) than that between suspended $\delta^{15}\text{N}_{\text{PON}}$ and $\delta^{15}\text{N}_{\text{NO}_3}$ ($\sim 9\text{--}10\text{‰}$) is consistent with some nitrogen recycling in the suspended particle pool.

Alternatively, the trapped sinking particles might have experienced some ^{15}N enrichment (e.g., via partial remineralization of source PON during their formation). Notably, the sinking particle $\delta^{15}\text{N}_{\text{PON}}$ values did not change throughout SOIREE, despite the clear increase in $\delta^{15}\text{N}_{\text{PON}}$ of the mixed-layer suspended particles (Fig. 2). This suggests that the ^{15}N -enriched PON in the fertilized mixed layer was not exported in a form that was caught in the traps, although it is possible that some was transferred to the submixed-layer suspended population and contributed to its apparent increase in $\delta^{15}\text{N}_{\text{PON}}$ in some size fractions over time (as discussed next).

Size-fractionated particle ^{15}N compositions—The size-fractionated suspended particles provide additional detail on the relationships between iron fertilization and nitrogen isotopic fractionation by phytoplankton. Outside the iron-fertilized waters, particles from the mixed layer at 30 m depth showed a monotonic increase in $\delta^{15}\text{N}_{\text{PON}}$ with increasing size, from $< -2\text{‰}$ in the 1–5- μm fraction to $> +0.5\text{‰}$ in the $> 200\text{-}\mu\text{m}$ fraction (Fig. 4a and Table 4 in Web Appendix 1). This increase also occurred within the iron-fertilized waters, but with the added feature of even higher $\delta^{15}\text{N}_{\text{PON}}$ (by 3–4‰) in the midsize fractions dominated by large, rapidly growing diatoms (Gall et al. 2001b; Trull and Armand 2001).

Below the surface mixed layer, the variation of $\delta^{15}\text{N}_{\text{PON}}$ with size was more complex, while still displaying many characteristics similar to those of the mixed-layer fractions. First, the submixed-layer (100 m) size fractions were almost universally ^{15}N -rich relative to the mixed-layer (30 m) size fractions (Fig. 4a,b and Table 4 in Web Appendix 1), both in and outside the iron-fertilized waters. This is consistent with the submixed-layer $\delta^{15}\text{N}_{\text{PON}}$ increase seen in the bulk suspended particle depth profiles and is probably a result of remineralization (Fig. 2). The submixed-layer particles also generally displayed increasing $\delta^{15}\text{N}_{\text{PON}}$ with increasing size, although this was not always true of the smallest size fraction. This fraction had a nearly 4‰ variation in $\delta^{15}\text{N}_{\text{PON}}$, perhaps reflecting the greater diversity of small particle sources at this depth, including small phytoplankton, fragments of larger sinking particles, and partially remineralized large particles.

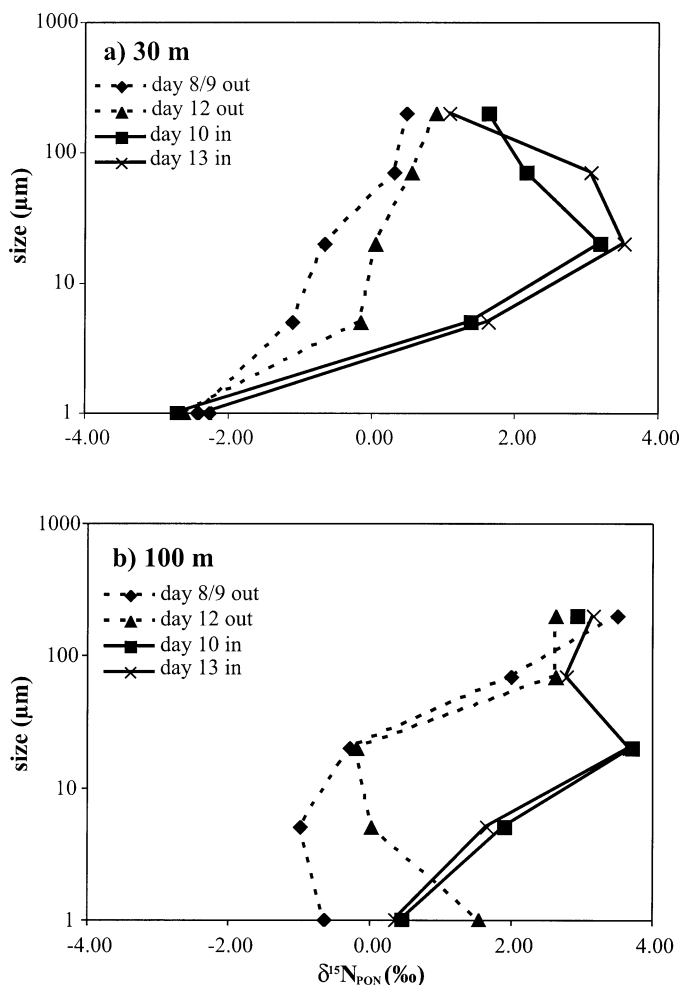


Fig. 4. $\delta^{15}\text{N}_{\text{PON}}$ variations with size from in- and out-patch at (a) 30 m and (b) 100 m. Note that size is plotted on a log scale. Size fractions 1–5, 5–20, 20–70, 70–200, and $>200 \mu\text{m}$ are represented by a data point at the smallest size in each fraction. Out-patch, $\delta^{15}\text{N}_{\text{PON}}$ generally increases with increasing size. In-patch, $\delta^{15}\text{N}_{\text{PON}}$ peaks dramatically in the midsize fractions (5–20, 20–70, 70–200 μm). Precision of $\delta^{15}\text{N}_{\text{PON}}$ values is 0.3‰.

Most surprisingly, the $\delta^{15}\text{N}_{\text{PON}}$ of midrange fractions (5–20 and 20–70 μm) was high in the samples from beneath the iron-fertilized waters in a similar fashion to the mixed-layer samples. The cause of this increase is unclear. As noted above, export to the traps from the mixed layer was negligible (Boyd et al. 2000; Nodder and Waite 2001; Trull and Armand 2001), little phytoplankton growth occurred at 100 m (Gall et al. 2001b), and there was no evidence for an iron-induced change in microbial activity (Hall and Safi 2001). Particle sinking and disaggregation could transfer mixed-layer particles to the submixed-layer suspended particle pool without an increase in export to the traps. It is also possible the $\delta^{15}\text{N}_{\text{PON}}$ variations in the 100-m size-fractionated samples derive from other sources, such as spatial or temporal variations in particle sources or the history of remineralization. (As noted in the Methods section, the samples taken from

outside the iron-fertilized waters varied considerably in their location.)

Discussion

The occurrence of elevated $\delta^{15}\text{N}_{\text{NO}_3}$ accompanying seasonal nitrate consumption and an increase in $\delta^{15}\text{N}_{\text{PON}}$ below the mixed layer in response to remineralization (Fig. 2) are well known (e.g., Altabet and McCarthy 1986; Sigman et al. 1999b), and the seasonal epsilon we calculate for the region is similar to recent studies (Altabet and François 2001). However, this is the first work to document $\delta^{15}\text{N}_{\text{PON}}$ variation with particle size in Southern Ocean samples and in relation to iron availability. We next consider these aspects in more detail, and speculate as to their possible origins. In doing so, we focus exclusively on the mixed-layer samples, where increased iron availability and its effects were unequivocal. We then examine how these results might affect interpretation of the $\delta^{15}\text{N}$ palaeoproxy in the Southern Ocean.

$\delta^{15}\text{N}_{\text{PON}}$ relation to particle size—A few studies have previously addressed variation in $\delta^{15}\text{N}_{\text{PON}}$ with plankton size in temperate waters. The $\delta^{15}\text{N}_{\text{PON}}$ of particles $>75 \mu\text{m}$ was found to be consistently $\sim 2\%$ higher than 1–75- μm particles in the surface layer of the Sargasso Sea (Altabet 1988). At a coastal Mediterranean site $\delta^{15}\text{N}_{\text{PON}}$ values ranged from -0.5 to $+5.7\%$ among size classes <3 , 3–8, 8–20, 20–150, and $>150 \mu\text{m}$ (Rau et al. 1990). Size fractions 8–20, 20–150, and $>150 \mu\text{m}$ exhibited the highest values. These results are similar to our results for the unfertilized Antarctic plankton community during SOIREE, but comparisons must be made with caution because, in the oligotrophic locations, nearly all of the phytoplankton is $<3 \mu\text{m}$ in size, and the larger fractions are dominated by heterotrophs.

Several processes could contribute to the $\delta^{15}\text{N}_{\text{PON}}$ increase with increasing size in the SOIREE plankton community. The largest SOIREE size fraction contained some copepods and pteropods that fed on small phytoplankton throughout the experiment (Zeldis 2001) and could be affected by heterotrophic ^{15}N enrichment. Trophic transfer of N results in an enrichment in $^{15}\text{N}_{\text{PON}}$ between the food source and consumer (e.g., DeNiro and Epstein 1981; Wada et al. 1987). The difference in $\delta^{15}\text{N}_{\text{PON}}$ between the largest size fraction ($>200 \mu\text{m}$) and smallest (1–5 μm) at both 30 and 100 m in this study approximates the average $\sim 3\%$ increase in ^{15}N composition per upward shift in trophic level (e.g., Wada et al. 1987).

During SOIREE, all size fractions $<200 \mu\text{m}$ were dominated by phytoplankton biomass; thus, some process other than heterotrophic enrichment must have contributed to their increase in $\delta^{15}\text{N}_{\text{PON}}$ with size. Variation in epsilon with cell size, growth rate, or species is a possible contributor. Laboratory and field studies of the potential relationship between growth rate and nitrogen isotopic fractionation have thus far proved equivocal (Wada and Hattori 1978; Montoya and McCarthy 1995; Rau et al. 1998). The variation with size might represent different biochemical mechanisms of nitrogen assimilation associated with the different diatom species that dominated the size fractions. Species-specific ^{15}N fractionation accompanying nitrate uptake has been documented by

Montoya and McCarthy (1995) between diatoms and dino-flagellates, but unfortunately, variations among diatom species have not been studied in any detail.

Assimilation of other nitrogen forms could also contribute to the $\delta^{15}\text{N}_{\text{PON}}$ variations with size. Studies in the Southern Ocean have documented that, despite nitrate concentrations $>20 \mu\text{mol L}^{-1}$, phytoplankton include regenerated nitrogen sources such as ammonium and urea as a large fraction of their N nutrition (e.g., Probyn and Painting 1985; Smith and Sakshaug 1990; Sambrotto and Mace 2000). Ammonium uptake contributes preferentially to primary production in the nanoplankton size class (2–20 μm), with nitrate being relatively more important for microplankton ($>20 \mu\text{m}$) nutrition (e.g., Probyn and Painting 1985) and particularly diatoms (Landry et al. 1997). Ammonium typically has a low $\delta^{15}\text{N}$ relative to nitrate because it derives from degraded PON (-2‰ at the start of SOIREE compared to 7.8‰ of nitrate), and additional depletion in ^{15}N accompanies its uptake by phytoplankton (e.g., Waser et al. 1998). Thus, preferential uptake of ammonium in the smaller size classes will lead to depleted $^{15}\text{N}_{\text{PON}}$ values relative to larger size classes that utilize a larger fraction of nitrate for their nitrogen nutrition. Unfortunately, concentrations and uptake of regenerated nitrogen forms were not measured during SOIREE. Based on the relatively small difference between $\delta^{15}\text{N}_{\text{NO}_3}$ of suspended and sinking particles at the start of SOIREE ($\sim 2\text{‰}$), ammonium uptake was a relatively small, but clearly present, influence on PON isotopic compositions. This small effect is consistent with the generally low concentrations of ammonium in open ocean Antarctic Zone waters (e.g., Sambrotto and Mace 2000).

Effects of iron on $\delta^{15}\text{N}_{\text{PON}}$ —The SOIREE iron fertilization spurred a shift to large diatoms ($>20 \mu\text{m}$), dominated by the species *Fragilariopsis kerguelensis* and *Dactyliosolen antarctica*. Their contribution to community primary production increased from 25% before iron enrichment to 60% by the end of the 13-d monitoring period (Gall et al. 2001b). The change in size distribution to more large cells (with high $\delta^{15}\text{N}_{\text{PON}}$ values relative to small cells before iron enrichment) can account for less than half of the increase in bulk $\delta^{15}\text{N}_{\text{PON}}$ that occurred by day 9, as shown in Fig. 5. The out-patch size-fractionated $\delta^{15}\text{N}_{\text{PON}}$ represents variation in $\delta^{15}\text{N}_{\text{PON}}$ with size without the effects of iron. Multiplying out-patch $\delta^{15}\text{N}_{\text{PON}}$ values by the biomass in each size fraction (as estimated from Chl *a* [Gall et al. 2001a]) yields the change in bulk $\delta^{15}\text{N}_{\text{PON}}$ driven by the shift in dominant size from pico- to microplankton during SOIREE, and this is only $\sim 40\%$ of the increase in bulk $\delta^{15}\text{N}_{\text{PON}}$ (Fig. 5). Thus, beyond its effect on dominant cell size, iron must affect $\delta^{15}\text{N}_{\text{PON}}$ more directly. In-patch size-fractionated $\delta^{15}\text{N}_{\text{PON}}$ values, those influenced by iron, when multiplied by changes in biomass, more closely approximate the observed temporal increase (Fig. 5). Iron is likely to have increased the $\delta^{15}\text{N}_{\text{PON}}$ of the size-fractionated and bulk PON by modifying the same parameters that produced the variations with size before fertilization: community structure, growth rate, and nitrogen source. Changes in the first two parameters implicate a change in the epsilon of nitrate fractionation; a change in nitrogen source does not.

If the increases stem from a change in epsilon, iron re-

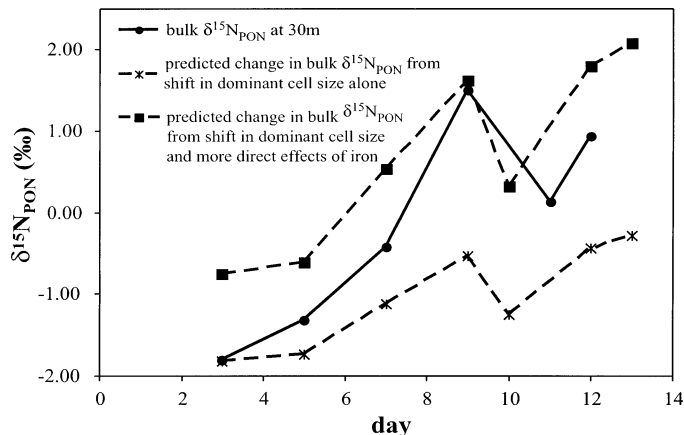


Fig. 5. The observed bulk $\delta^{15}\text{N}_{\text{PON}}$ increase over time requires contributions from both changes in dominant phytoplankton size and more direct effects of iron addition. Estimating the effect of size increase alone by combining the out-patch size-fractionated $\delta^{15}\text{N}_{\text{PON}}$ 30-m results with temporal increases in size-fractionated biomass based on Chl *a* at 40 m (Gall et al. 2001a) yields an increase in bulk $\delta^{15}\text{N}_{\text{PON}}$ over time but is insufficient to account for the full magnitude of the observed increase in bulk $\delta^{15}\text{N}_{\text{PON}}$. The more direct effects of iron, included by combining the in-patch size fraction $\delta^{15}\text{N}_{\text{PON}}$ 30-m results with the Chl *a* data, are required to approximate the observed temporal increase in bulk $\delta^{15}\text{N}_{\text{PON}}$. The Chl *a* measurements were on size fractions 0.2–2, 2–5, 5–20, and $>20 \mu\text{m}$, which we assigned $\delta^{15}\text{N}_{\text{PON}}$ values of -3.0‰ , -2.5‰ , -0.75‰ , and 0.50‰ , respectively, for outside the patch and -3.0‰ , -2.5‰ , 1.6‰ , and 3.5‰ , respectively, for inside the patch based on our results shown in Fig. 4. We used an algal C:Chl *a* ratio of 140 (Gall et al. 2001a) and a Redfield C:N ratio of 6.7.

duced the apparent ϵ estimated from the offset between bulk $\delta^{15}\text{N}_{\text{PON}}$ and $\delta^{15}\text{N}_{\text{NO}_3}$ (Eq. 2) from $8\text{--}9\text{‰}$ to $\sim 6\text{‰}$ (Fig. 2). For the large diatoms (20–70 and 70–200 μm) that dominated the bloom, ϵ estimated in this way reached values as low as 4.5‰ . A change in epsilon could derive from changes in algal community structure or growth rate. Changes in SOIREE community structure were examined through cell counts and estimated relative abundances of the major diatom species present in the size classes before and after iron enrichment (see data presented in Trull and Armand 2001). Although the species *F. kerguelensis* and *D. antarctica* (which dominated the 20–70- and 70–200- μm size classes that exhibited the greatest response to iron [Fig. 4]) were both present at $>20\%$ before iron addition, their increase in relative abundance in the iron-induced bloom could have affected bulk $\delta^{15}\text{N}_{\text{PON}}$ if these species fractionate nitrate with an ϵ significantly different to other species within their size classes. The 20–70- μm fraction that showed the most dramatic increase in $\delta^{15}\text{N}_{\text{PON}}$ with iron addition was comprised almost entirely ($\sim 90\%$) of these two species.

Algal growth rates within the iron-fertilized waters increased 10-fold from an initial $\sim 0.02 \text{ d}^{-1}$ to $\sim 0.2 \text{ d}^{-1}$. The maximum in $^{15}\text{N}_{\text{PON}}$ values echoed the peak in community growth rates (Fig. 3). The lag time of $\sim 4 \text{ d}$ could reflect the time required for PON formed after the growth rate increase to replace PON formed prior to iron fertilization. Growth rates of the size fractions with elevated $^{15}\text{N}_{\text{PON}}$ (microplank-

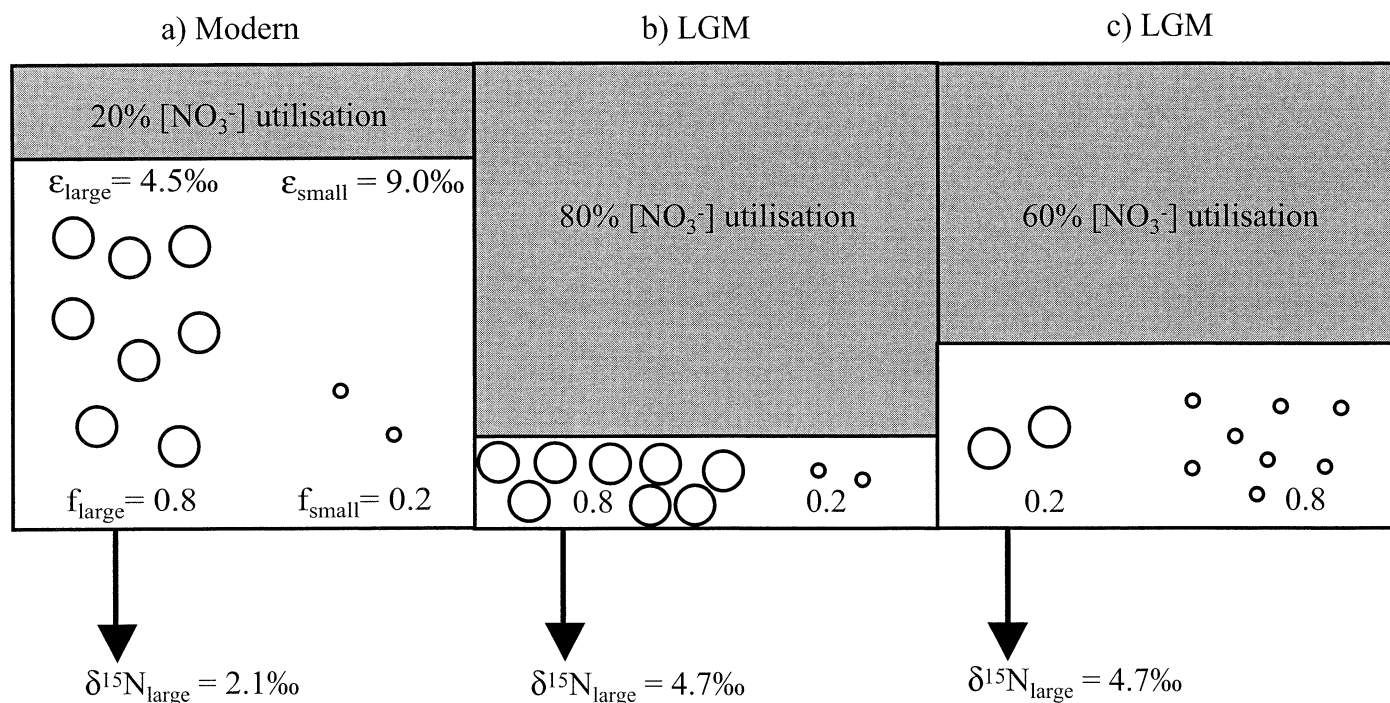


Fig. 6. An example of the effects of community change on scaling $\delta^{15}\text{N}_{\text{PON}}$ of a specific component of sediment (e.g., diatom-bound nitrogen) to nitrate utilization. (a) The Modern situation reflects the current estimated 20% utilization of the Antarctic Zone nitrate pool and the large fraction of large diatoms relative to small cells in exported organic material. (b) To generate the $\sim 1\text{--}4\text{‰}$ increase from Modern to LGM in $\delta^{15}\text{N}_{\text{PON}}$ of diatoms (here, 2.6‰) requires a fourfold increase in nitrate utilization with no community change. (c) If the LGM community contained a larger fraction of small cells, only an approximate twofold increase in utilization is required. Values were generated using Eqs. 4 and 5 and are displayed in Table 1.

ton [$>20\ \mu\text{m}$] and nanoplankton [$2\text{--}20\ \mu\text{m}$]) were consistently higher than those of smaller phytoplankton after day 6 (Gall et al. 2001b). As reviewed above, the role of growth rate in nitrogen isotopic fractionation is not yet clear.

An iron-induced shift to greater reliance on nitrate in comparison to ammonium could also (or alternatively) have contributed to the high $\delta^{15}\text{N}_{\text{PON}}$ within the larger size classes. In Southern Ocean incubation experiments, the addition of iron led to enhanced nitrate reductase activity and nitrate uptake with no change in ammonium uptake (Timmermans et al. 1998) (phytoplankton use the iron-containing enzymes nitrate reductase and nitrite reductase to reduce and assimilate nitrate, whereas regenerated forms of nitrogen such as ammonium are already reduced). The effect of iron shows a size dependence: iron-induced nitrate uptake increases were confined to large phytoplankton (defined as $>3\ \mu\text{m}$ in the study) in Southern Ocean culture studies, with small phytoplankton unaffected in NO₃⁻ uptake rate and biomass by Fe enrichment (Price et al. 1994). Iron addition leads to increased nitrate uptake rates in large cells and thus higher $\delta^{15}\text{N}_{\text{PON}}$ values relative to smaller cells that continue to use ammonium.

Scaling sedimentary $\delta^{15}\text{N}_{\text{PON}}$ to nitrate utilization—In the Antarctic, the $\delta^{15}\text{N}$ of last glacial maximum (LGM) sediments was 1–4‰ higher than modern sediments (François et al. 1992, 1997). This magnitude of change has also been observed in diatom frustule-associated organic matter, con-

firming that it is not a diagenetic effect (Sigman et al. 1999a). Based on the assumption of a constant ϵ , this change has been interpreted to suggest that nitrate utilization during the last ice age was from two to four times its current value (François et al. 1997; Sigman et al. 1999a), a shift that a simple box model suggests could lower atmospheric CO₂ by the full glacial/interglacial amplitude (Sigman et al. 1999a). Higher dust deposition during the LGM could have led to higher iron availability (Martin 1990; Mahowald et al. 1998), and the SOIREE results suggest that ϵ might vary with iron availability either directly or via increases in mean phytoplankton size. If the LGM iron inputs induced lower ϵ values by 2‰ (e.g., from 8 to 6‰ as suggested by the SOIREE results), then the higher $\delta^{15}\text{N}$ of LGM sediments implies that nitrate utilization in the LGM was closer to one to three times modern values.

The effect of possible ecosystem-driven changes in ϵ on the interpretation of the sediment record depends also on whether all phytoplankton contribute to the record. It is possible that large diatoms contribute preferentially to Antarctic sediments. Species such as the heavily silicified *F. kerguelensis* (which dominated the SOIREE bloom) resist dissolution and appear to dominate sediment assemblages (e.g., Shemesh et al. 1989). If components of the phytoplankton community contribute preferentially to sediment assemblages, then the effect of community change on the scaling of sedimentary $\delta^{15}\text{N}$ changes to nitrate utilization is more complex.

Table 1. Calculation of nitrate utilization as defined in Eq. 1 required to yield a 1–4‰ increase in large-diatom $\delta^{15}\text{N}_{\text{PON}}$ from modern sediments to LGM with and without a change in community composition. $\delta^{15}\text{N}_{\text{NO}_3\text{initial}} = 6.0\text{‰}$ (based on isotopic composition of upper circumpolar deep water [UCDW]) (Sigman et al. 1999b), large-diatom $\varepsilon = 4.5\text{‰}$, and small-cell $\varepsilon = 9.0\text{‰}$ (based on results of this study). In the modern Southern Ocean, where nitrate utilization is $\sim 20\%$ and large diatoms dominate the phytoplankton community (large-diatom fraction, 0.8) large-diatom $\delta^{15}\text{N}_{\text{PON}}$ ranges from $\sim 2.1\text{--}2.8\text{‰}$. To account for the observed increase in diatom $\delta^{15}\text{N}_{\text{PON}}$ from interglacial to glacial periods observed in studies using the diatom-bound proxy (1–4‰, here 2.6‰), there must be about a fourfold increase in nitrate utilization with no change in community composition, but only about a two- to threefold increase in utilization if community dominance in the LGM shifts from the modern large diatoms (large-diatom fraction, 0.8) to smaller cells (large-diatom fraction, 0.2).

Time	Utilization (%)	Fraction of large diatoms	ε community (‰)	$\delta^{15}\text{N}_{\text{PON}}$ large diatoms (‰)	$\delta^{15}\text{N}_{\text{PON}}$ small cells (‰)	$\delta^{15}\text{N}_{\text{PON}}$ community (‰)	$\delta^{15}\text{N}_{\text{NO}_3}$ (‰)
Modern	40	0.8	5.4	2.8	−1.7	1.9	8.8
Modern	30	0.8	5.4	2.4	−2.1	1.5	7.9
Modern	20	0.8	5.4	2.1	−2.4	1.2	7.2
LGM	60	0.2	8.1	4.7	0.2	1.1	13.4
LGM	80	0.8	5.4	4.7	0.2	3.8	14.7

To illustrate this, Fig. 6 shows a cartoon of how community changes could account for about half of the observed glacial to modern changes in the $\delta^{15}\text{N}$ of the sedimentary record of diatom-associated organic matter. This could occur if the LGM phytoplankton community had a much greater proportion of small phytoplankton in comparison to modern Antarctic Zone assemblages (as might occur in a sea ice-covered LGM Antarctic Zone), but only large diatoms contributed importantly to the sedimentary record. Table 1 shows accumulated product values of $\delta^{15}\text{N}_{\text{PON}}$ calculated separately for large and small cells (with an ε of 4.5 and 9‰, respectively, as observed during SOIREE) from

$$\delta^{15}\text{N}_{\text{PON}_i} = \delta^{15}\text{N}_{\text{NO}_3\text{initial}} - \varepsilon_c \{(1 - u)/u\} \ln(1 - u) + (\varepsilon_c - \varepsilon_i) \quad (4)$$

in which ε_i applies to each size and ε_c is the fractionation factor for the community calculated from

$$\varepsilon_c = \sum f_i \varepsilon_i \quad (5)$$

where the f_i are the fractions of total nitrate taken up by each size class. (Equation 4 is derived by substituting Eq. 1 written for the whole community [ε_c] into Eq. 2 written for a size class characterized by ε_i , and then integrated to obtain the accumulated product $\delta^{15}\text{N}_{\text{PON}}$ for the size class i .)

For the observed modern high-nitrate waters of the Antarctic Zone (which experience $\sim 20\%$ nitrate utilization [e.g., Altabet and François 2001]), a mix of 20% small phytoplankton and 80% large phytoplankton provides good agreement with both the observed SOIREE size-fractionated range of $\delta^{15}\text{N}_{\text{PON}}$ and observations of $\sim 2\text{‰}$ for $\delta^{15}\text{N}$ of diatom-bound organic matter in modern sediments (Fig. 6a). To obtain the higher $\delta^{15}\text{N}$ of $\sim 5\text{‰}$ for diatom-bound organic matter in LGM sediments (Sigman et al. 1999a) requires about four times greater nutrient depletion (i.e., nitrate utilization of 80%) if no community change is assumed (Fig. 6b), but an increase to only 60% nitrate utilization if smaller cells were more abundant (80% of the community) in a sea ice-covered LGM Antarctic Zone (Fig. 6c). We are not arguing that this community change is known to have occurred

(little data on cell sizes is available, and then only for those species that leave well-preserved shells). The point is that the scaling of sedimentary $\delta^{15}\text{N}$ to nitrate utilization depends on both phytoplankton community structure and on which components of the phytoplankton community dominate the sedimentary record. Moreover, it is not just the magnitude of the scaling that is affected, but also the direction. As seen in this example, if large diatoms control the sedimentary record, then more small phytoplankton in the community leads to higher sedimentary $\delta^{15}\text{N}$. If all phytoplankton contribute equally to the record, more small phytoplankton in the community leads to lower sedimentary $\delta^{15}\text{N}$.

As more studies address the size, species, growth rate, and nitrogen source effects on the $\delta^{15}\text{N}$ of PON, it will become possible to couple these results with other proxies for community structure to develop more sophisticated interpretations of LGM nutrient dynamics in the Southern Ocean. Key studies to further this approach include (1) determining the variations of $\delta^{15}\text{N}$ with cell size in spring, when ammonium contributions are likely to be minimal (and can be determined), so that the role of changes in nitrogen source can be separated from cell size and growth rate variations, and (2) examining exported materials to better understand the degree to which mixed-layer nitrogen recycling affects the scaling between nitrate utilization and the $\delta^{15}\text{N}$ of PON. In that regard, recent studies have shown that exported PON in the Southern Ocean does not always display the seasonal cycle expected for nitrate-controlled export production (Van Hale 2002; Lourey unpubl. data), although annual averages might escape this problem (Altabet and François 2001). Focusing on large diatoms in these studies remains important because large diatoms ($>20 \mu\text{m}$) dominate biogenic flux to the sediments in the Southern Ocean and are thought to drive burial of organic carbon now and in the past (Kumar et al. 1995; de Baar and Boyd 1999).

References

- ALTABET, M. A. 1988. Variations in nitrogen isotopic composition between sinking and suspended particles: Implications for ni-

- trogen cycling and particle transformation in the open ocean. *Deep-Sea Res.* **35**: 535–554.
- , AND R. FRANÇOIS. 1994. Sedimentary nitrogen isotopic ratio as a recorder for surface ocean nitrate utilization. *Glob. Biogeochem. Cycles* **8**: 103–116.
- , AND ———. 2001. Nitrogen isotope biogeochemistry of the Antarctic Polar Frontal Zone at 170 W. *Deep-Sea Res. II—Top. Stud. Oceanogr.* **48**: 1–27.
- , AND J. J. MCCARTHY. 1986. Vertical patterns in ^{15}N natural abundance in PON from the surface waters of warm-core rings. *J. Mar. Res.* **44**: 185–201.
- BOYD, P. W., AND OTHERS. 2000. A mesoscale phytoplankton bloom in the polar Southern Ocean stimulated by iron fertilization. *Nature* **407**: 695–702.
- DE BAAR, H. J. W., AND P. W. BOYD. 1999. The role of iron in plankton ecology and carbon dioxide transfer of the global oceans, p. 61–140. *In* R. B. Hanson, H. W. Ducklow, and J. G. Field [eds.], *The dynamic ocean carbon cycle: A midterm synthesis of the Joint Global Ocean Flux Study*. Cambridge Univ. Press.
- DENIRO, M. J., AND S. EPSTEIN. 1981. Influence of diet on the distribution of nitrogen isotopes in animals. *Geochim. Cosmochim. Acta* **45**: 341–351.
- FRANÇOIS, R., M. A. ALTABET, AND L. H. BURCKLE. 1992. Glacial to interglacial changes in surface nitrate utilization in the Indian sector of the Southern Ocean as recorded by sediment $\delta^{15}\text{N}$. *Paleoceanography* **7**: 589–606.
- , AND OTHERS. 1997. Contribution of Southern Ocean surface-water stratification to low atmospheric CO_2 concentrations during the last glacial period. *Nature* **389**: 929–935.
- FREW, R., A. BOWIE, P. CROOT, AND S. PICKMERE. 2001. Macro-nutrient and trace-metal geochemistry of an in situ iron-induced Southern Ocean bloom. *Deep-Sea Res. II—Top. Stud. Oceanogr.* **48**: 2467–2481.
- GALL, M. P., P. W. BOYD, J. HALL, K. A. SAFI, AND H. CHANG. 2001a. Phytoplankton processes. Part 1: Community structure during the Southern Ocean Iron Release Experiment (SOIREE). *Deep-Sea Res. II—Top. Stud. Oceanogr.* **48**: 2551–2570.
- , R. STRZEPEK, M. MALDONADO, AND P. W. BOYD. 2001b. Phytoplankton processes. Part 2. Rates of primary production and factors controlling algal growth during the Southern Ocean Iron Release Experiment (SOIREE). *Deep-Sea Res. II—Top. Stud. Oceanogr.* **48**: 2571–2590.
- HALL, J. A., AND K. SAFI. 2001. The impact of in situ Fe fertilisation on the microbial food web in the Southern Ocean. *Deep-Sea Res. II—Top. Stud. Oceanogr.* **48**: 2591–2613.
- HANNON, E., P. W. BOYD, M. SILVOSO, AND C. LANCELOT. 2001. Modeling the bloom evolution and carbon flows during SOIREE: Implications for future in situ iron-enrichments in the Southern Ocean. *Deep-Sea Res. II—Top. Stud. Oceanogr.* **48**: 2745–2773.
- KUMAR, N., R. F. ANDERSON, R. A. MORTLOCK, P. N. FROELICH, P. KUBIK, B. DITTRICHMANNEN, AND M. SUTER. 1995. Increased biological productivity and export production in the glacial Southern Ocean. *Nature* **378**: 675–680.
- LANDRY, M. R., AND OTHERS. 1997. Iron and grazing constraints on primary production in the central equatorial Pacific: An EqPac synthesis. *Limnol. Oceanogr.* **42**: 405–418.
- LOUREY, M. J., AND T. W. TRULL. 2001. Seasonal nutrient depletion and carbon export in the Subantarctic and Polar Frontal Zones of the Southern Ocean south of Australia. *J. Geophys. Res.* **106**: 31,463–31,488.
- MAHOWALD, N., AND OTHERS. 1998. Dust sources and deposition during the last glacial maximum and current climate: A comparison of model results with paleodata from ice cores and marine sediments. *J. Geophys. Res. [Atmos.]* **104**: 15,895–15,916.
- MARTIN, J. H. 1990. Glacial-interglacial CO_2 change: The iron hypothesis. *Paleoceanography* **5**: 1–13.
- MONTOYA, J. P., AND J. J. MCCARTHY. 1995. Isotopic fractionation during nitrate uptake by phytoplankton grown in continuous culture. *J. Plankton Res.* **17**: 439–464.
- NODDER, S. D., AND A. M. WAITE. 2001. Is Southern Ocean organic carbon and biogenic silica export enhanced by iron-stimulated increases in biological production? Sediment trap results from SOIREE. *Deep-Sea Res. II—Top. Stud. Oceanogr.* **48**: 2681–2702.
- PRICE, N. M., B. A. AHNER, AND F. M. M. MOREL. 1994. The equatorial Pacific Ocean: Grazer-controlled phytoplankton populations in an iron-limited ecosystem. *Limnol. Oceanogr.* **39**: 520–534.
- PROBYN, T. A., AND S. J. PAINTING. 1985. Nitrogen uptake by size-fractionated phytoplankton populations in Antarctic surface waters. *Limnol. Oceanogr.* **30**: 1327–1332.
- RAU, G. H., J.-L. TEYSSIE, F. RASSOULZADEGAN, AND S. W. FOWLER. 1990. $^{13}\text{C}/^{12}\text{C}$ and $^{15}\text{N}/^{14}\text{N}$ variations among size-fractionated marine particles: Implications for their origin and trophic relationships. *Mar. Ecol. Prog. Ser.* **59**: 33–38.
- , C. LOW, J. T. PENNINGTON, K. R. BUCK, AND F. P. CHAVEZ. 1998. Suspended particulate nitrogen $\delta^{15}\text{N}$ versus nitrate utilization: Observations in Monterey Bay, CA. *Deep-Sea Res. II—Top. Stud. Oceanogr.* **45**: 1603–1616.
- SAINO, T., AND A. HATTORI. 1980. ^{15}N natural abundance in oceanic suspended particulate matter. *Nature* **283**: 752–754.
- SAMBROTTO, R. N., AND B. J. MACE. 2000. Coupling of biological and physical regimes across the Antarctic Polar Front as reflected by nitrogen production and recycling. *Deep-Sea Res. II—Top. Stud. Oceanogr.* **47**: 3339–3367.
- SHEMESH, A., L. H. BURCKLE, AND P. N. FROELICH. 1989. Dissolution and preservation of Antarctic diatoms and the effect on sediment thanatocoenoses. *Quat. Res.* **31**: 288–308.
- SIGMAN, D. M., M. A. ALTABET, R. FRANÇOIS, D. C. MCCORKLE, AND J. F. GAILLARD. 1999a. The isotopic composition of diatom-bound nitrogen in Southern Ocean sediments. *Paleoceanography* **14**: 118–134.
- , ———, D. C. MCCORKLE, R. FRANÇOIS, AND G. FISCHER. 1999b. The $\delta^{15}\text{N}$ of nitrate in the Southern Ocean: Consumption of nitrate in surface waters. *Glob. Biogeochem. Cycles* **13**: 1149–1166.
- , K. L. CASCIOTTI, M. ANDREANI, C. BARFORD, M. GALANTER, AND J. K. BOHLKE. 2001. A bacterial method for the nitrogen isotopic analysis of nitrate in seawater and freshwater. *Anal. Chem.* **73**: 4145–4153.
- SMITH, W. O., JR., AND E. SAKSHAUG. 1990. Polar phytoplankton, p. 477–525. *In* W. O. Smith Jr. [ed.], *Polar oceanography part B: Chemistry, biology, and geology*. Academic.
- TIMMERMANS, K. R., AND OTHERS. 1998. Iron stress in the Pacific region of the southern ocean—evidence from enrichment bioassays. *Mar. Ecol. Prog. Ser.* **166**: 27–41.
- TRULL, T. W., AND L. ARMAND. 2001. Insights into Southern Ocean carbon export from the $\delta^{13}\text{C}$ of particles and dissolved inorganic carbon during the SOIREE iron release experiment. *Deep-Sea Res. II—Top. Stud. Oceanogr.* **48**: 2655–2680.
- , S. R. RINTOUL, M. HADFIELD, AND E. R. ABRAHAM. 2001. Circulation and seasonal evolution of polar waters south of Australia: Implications for iron fertilization of the Southern Ocean. *Deep-Sea Res. II—Top. Stud. Oceanogr.* **48**: 2439–2466.
- VAN HALE, R. J. 2002. Stable isotope biogeochemistry of the Otago continental shelf. Ph.D. thesis, Otago Univ., Dunedin, New Zealand.

- WADA, E., AND A. HATTORI. 1978. Nitrogen isotope effects in the assimilation of inorganic nitrogenous compounds by marine diatoms. *Geomicrobiol. J.* **1**: 85–101.
- , M. TERAZAKI, Y. KABAYA, AND T. NEMOTO. 1987. ^{15}N and ^{13}C abundances in the Antarctic Ocean with emphasis on the biogeochemical structure or the food web. *Deep-Sea Res.* **34**: 829–841.
- WASER, N. A. D., P. J. HARRISON, B. NIELSEN, S. E. CALVERT, AND D. H. TURPIN. 1998. Nitrogen isotope fractionation during the uptake and assimilation of nitrate, nitrite, ammonium, and urea by a marine diatom. *Limnol. Oceanogr.* **43**: 215–224.
- ZELDIS, J. 2001. Mesozooplankton community composition, feeding, and export production during SOIREE. *Deep-Sea Res. II—Top. Stud. Oceanogr.* **48**: 2615–2634.

Received: 8 February 2002

Accepted: 17 September 2002

Amended: 21 November 2002